Eng. Sci., 2022, **18**, 187–192

Engineered Science

DOI: https://dx.doi.org/10.30919/es8d498

Tunable Terahertz Perfect Absorber Based on Graphene-Photonic Crystal Hetero-Structure

Jun Wu*

Abstract

The perfect absorption in monolayer graphene at terahertz frequencies is investigated. The designed absorber consists of a monolayer graphene separated from a dielectric multilayer structure by a dielectric film. Nearly 100% absorption is observed at resonance, which results from the excitation of graphene Tamm plasmon polaritons at the boundary between the graphene and dielectric multilayer. The distribution of the electric field intensity along the *z*-axis is also presented to disclose the physical origin of such a perfect absorption phenomenon. Besides, the operating frequencies can be flexibly tuned by changing the angle of incidence, which is particularly attractive as the graphene absorption is not sensitive to the polarization state. Furthermore, the absorption properties can be maintained with large fabrication tolerance, which is an advantage for practical fabrication. Lastly, it is found that the operating frequency can be easily tuned by a change in the gate voltage. It is believed the conclusions provide the potential for combining graphene with metamaterial to enable novel THz tunable device applications.

Keywords: Graphene; Metamaterial; Absorption; Plasmonic; Tunable.
Received: 30 June 2021; Revised: 17 July 2021; Accepted: 01 August 2021.
Article type: Research article.

1. Introduction

As a kind of functional device, terahertz absorbers have received increasing attention recently, owing to their potential applications in various fields such as sensors,[1,2] detectors,[3] medical imaging[4,5], and stealth technology.[6] Therefore, in the past few years, many novel methods have been proposed to achieve perfect THz absorption by employing various structures and materials, including epsilon-near-zero structures with hyperbolic dispersion,[7] photonic crystal structure,[8] metamaterial,[9] and metasurface.[10] Among these, metal-insulator-metal (MIM) structures are the typical components of many THz absorbers. But these absorbers are static, whose performances solely depend on their structural parameters. The dynamic controlling of THz absorbers is highly desirable, which has prompted the development of several techniques, including liquid crystals,[11] microelectromechanical systems,[12] and graphene.[13] Among these, graphene is an important and potential candidate to realize perfect tunable absorption at terahertz frequency.

Graphene, as a monolayer of hexagonally arranged carbon atoms have attracted a lot of attention due to their unprecedented optical and electric properties.[14-16] First, thanks to its two-dimensional property, the strong plasmonic response can be excited, leading to a strong light-graphene interaction with extremely light confinement to the interface.[17,18] Moreover, its conductivity can be tuned by controlling the gate voltage upon graphene.[19] Such characteristics have enabled graphene a key component in designing various kinds of devices such as infrared metamaterials and transformation optical devices,[20] perfect tunable absorbers,[21,22] modulating and detecting devices,[23,24] image devices,[25] waveguide,[26] and biosensors,[27], *etc*. Nevertheless, the optical absorption in the graphene monolayer is typically extremely low, which limits its substantial applications in the THz frequency range. Therefore, it is highly desirable to boost the absorption of an electromagnetic wave in the monolayer graphene. To solve this problem, various schemes have been designed recently to boost the THz absorption in monolayer graphene, such as combined metallic resonators with structured double graphene sheets,[28] graphene-based heterostructures,[29] patterned graphene-dielectric multilayers-metal mirror structures,[30] deposited graphene on a spacer layer backed by a mirror,[31] a tunable strength multiband absorber based on graphene circular rings,[32] realizing multichannel tunable perfect absorption based on a graphene-1D photonic crystal

College of Electrical Engineering, Anhui Polytechnic University, Wuhu 241000, China.
**Email:* mailswj2011@163.com (J. Wu)

structure.[33] However, searching for novel schemes and configurations to combine graphene into metamaterials to achieve tunable perfect absorption in the THz range is still highly desirable.

In this work, the perfect absorption in monolayer graphene at the THz frequency based on graphene Tamm plasmon polaritons is investigated, which is organized as follows. First, a perfect tunable THz absorber, in the form of a monolayer graphene placed on a dielectric multilayer structure separated by a spacer, is designed. Second, the distribution of the electric field intensity along the *z*-axis is illustrated to provide a physical understanding of this phenomenon. Next, the effects of the incident angle and the geometric parameters of the absorber on the absorption spectra are calculated and investigated, to guide tuning the operating frequency and device fabrication. Last it is shown that the perfect absorption properties can be flexibly tuned by applying external gate voltages. It is hoped that the conclusions should be valuable in the development of novel tunable devices based on graphene.

2. Design and analysis of the graphene absorber

The schematic of the designed THz absorber is presented in Fig. 1. The absorber is composed of a graphene monolayer coated upon a multilayer structure of two different materials separated by a spacer. The total structure can be assumed to be fabricated on a substrate S. Thus, the proposed absorber can be denoted as $GC(BA)^n(AB)^nS$, where C is the spacer between the monolayer graphene and the multilayer structure. Its thickness and refractive index are h_1 and 1.45, respectively. The multilayer structure we considered contains repeating two dielectric media A and B, arranged in the form of $F(n) = (BA)^n(AB)^n$ (n is a positive integer denoted as the sequence order). Their refractive indices are $n_a = 1.45$ and $n_b = 3.48$, respectively, with the corresponding thicknesses h_a and zHB, respectively. The refractive index of the substrate is selected as $n_s = 1.45$.

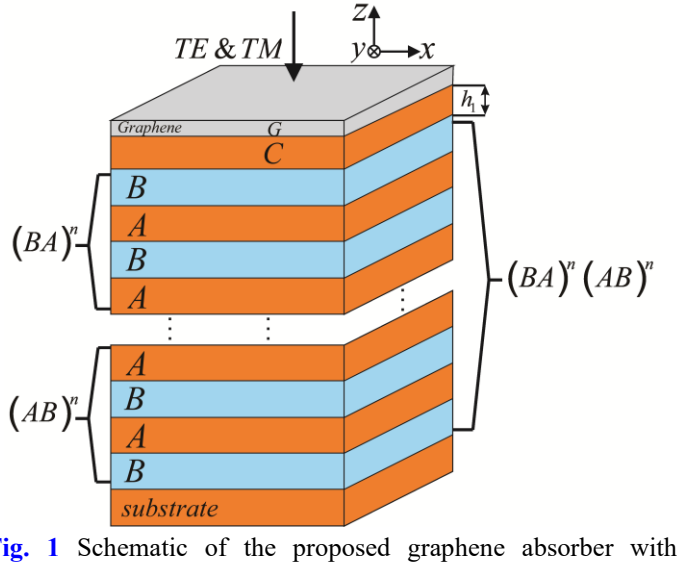

Fig. 1 Schematic of the proposed graphene absorber with multilayer structure $GC(BA)^n(AB)^nS$.

At the THz frequencies, the complex surface conductivity of graphene is simplified as a Drude-like term:[34,35]

$$\sigma(\omega) = \frac{e^2 E_f}{\pi\hbar^2}\frac{i}{\omega + i\tau^{-1}} \quad (1)$$

where $\hbar$ is the reduced Planck's constant and $E_f = 0.75$ eV denotes the Fermi level, ω denotes the angular frequency, e denotes the basic electric charges, and $\tau = 1.0$ *ps* is the carrier relaxation lifetime.

During the calculation, the monolayer graphene is considered a thin film with an equivalent permittivity:

$$\varepsilon_g = 1 + \frac{i\sigma(\omega)}{\varepsilon_0 \omega h_g} \quad (2)$$

where ε_0 denotes the relative permittivity of vacuum, and $h_g = 0.34$ nm is the thickness of the graphene monolayer.

To simulate the optical performance of the proposed device, the rigorous coupled-wave analysis (RCWA) was employed to obtain the reflection (R) and transmission (T) first.[36,37] Then the absorption (A) is calculated according to $A \equiv 1\text{-}R\text{-}T$. The detailed structure dimensions of the designed absorber are $n = 3$, $h_1 = 105$ μm, $h_a = 35$ μm and $h_b = 30$ μm. For normal incident light, the absorption spectra of TE-polarized (with the electric field along the direction of the y-axis) and TM-polarized (with the magnetic field along the direction of the y-axis) lights are the same due to the symmetry of the structure. Therefore, for light under normal incidence, we only take into account the TE-polarized wave. In Fig. 2, we show the calculated absorption spectra for the TE-polarized light under normal incidence. From the figure, two main points can be founded. First, nearly 100% light absorption is achieved at the resonant frequency of 0.89 THz, indicating that perfect absorption in the monolayer graphene is realized. Second, the bandwidth of the resonant peak is approximately 0.037 THz with the corresponding quality factor ($Q = f/\Delta f$) of about 24, which presents a narrow frequency bandwidth.

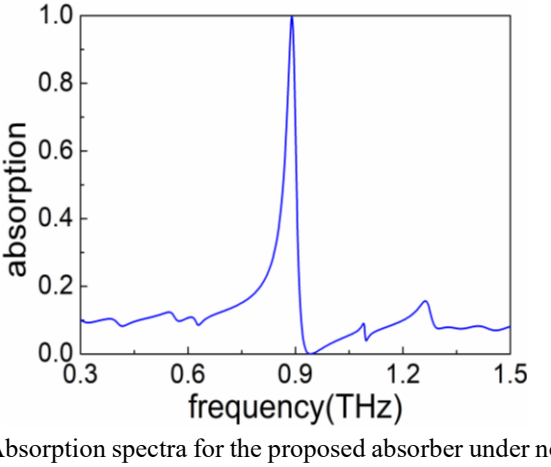

Fig. 2 Absorption spectra for the proposed absorber under normal incidence.

To qualitatively investigate the physical origin behind this perfect absorption effect, the normalized electric field intensity and the electric field intensity profile along the *z*-axis at the resonant frequency for the absorber with and without the covering of graphene are simulated and shown in Fig. 3. As presented in Figs. 3(a) and 3(b), the electric field intensity

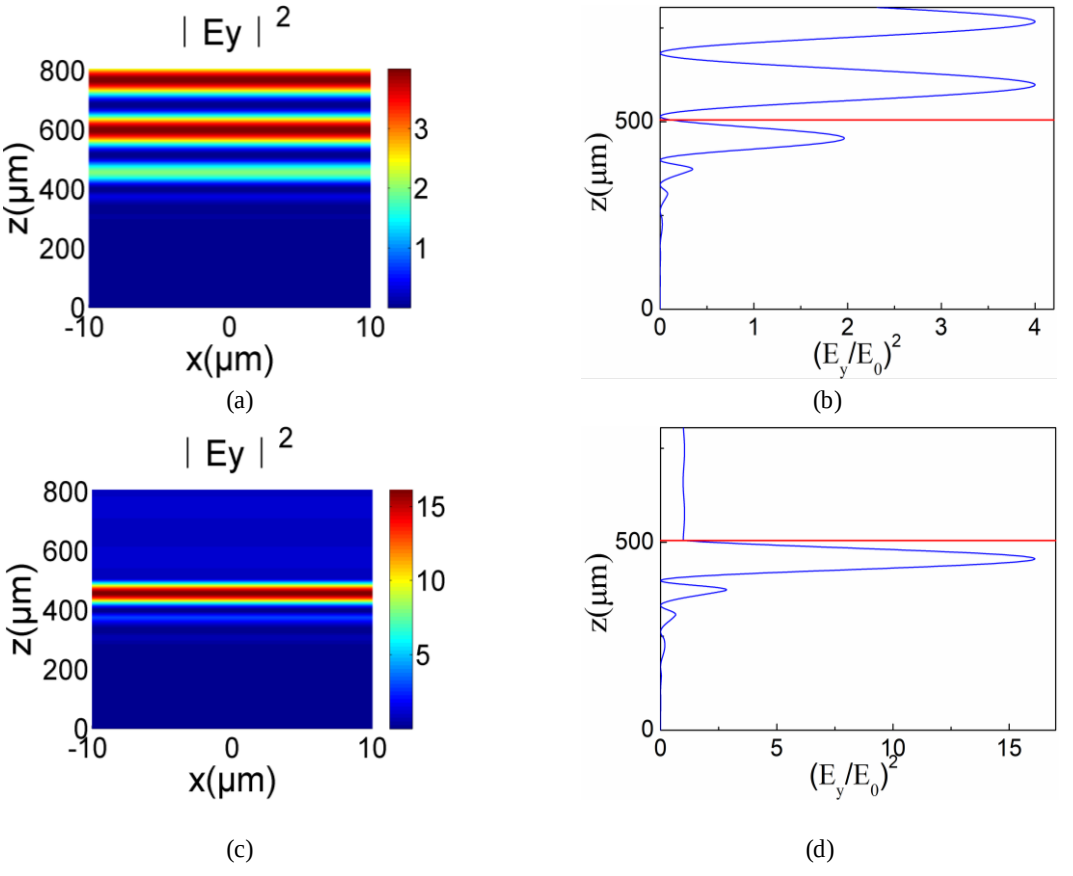

Fig. 3 (a) Normalized electric field intensity distributions and (b) intensity profile along the *z*-axis at 0.89 THz for the absorber without the depositing of graphene; (c) normalized electric field intensity distributions and (d) intensity profile for the absorber with the covering of graphene; the red solid line denotes the interface between air and spacer, where monolayer graphene is coated.

in the incident, the region presents a typical feature of the standing wave, which results from the superposition of the reflected wave and the incident wave. This indicates that nearly total reflection is achieved at the boundary between the incident media and the dielectric multilayer structure. At the same time, the electric field intensity decays exponentially in the dielectric multilayers. Moreover, the enhancement of the electric field intensity at the interface between the air and the dielectric multilayers is extremely weak. However, when monolayer graphene is placed on the dielectric multilayer structure, the electric field intensity at the resonant frequency is strongly enhanced and mainly confined in the spacer between graphene and the dielectric multilayers, as clearly illustrated in Figs. 3(c) and 3(d). This is attributed to the excitation of graphene TPPs. TPPs are a recently discovered surface wave, which is confined between two different layered material interfaces after excited.[38,39] In contrast to the surface plasmon polaritons, i.e. a kind of traditional surface wave, TPPs can be excited by either TE-polarized wave or TM-polarized wave without the assistance of external photonic structures.[40] Thus, the strongly enhanced electric field intensity below graphene can significantly promote light absorption in the monolayer graphene, which provides the possibility to achieve perfect absorption. This is also demonstrated by the intensity profile in the air where almost no reflected wave can be found. Thus, the perfect absorption in the monolayer graphene results from the excitation of the graphene TPPs.

3. Discussion

Typically, with the incident light deviating from normal incidence, the absorption spectra for TE-polarized and TM-polarized waves become different owing to the break of symmetry. Subsequently, the dependence of the light absorption in graphene on the incident angle is investigated. The simulated absorption spectra versus the change of frequency and the incident angle for TE-polarized and TM-polarized waves are shown in Figs. 4(a) and 4(b), respectively. The frequencies of the absorption peaks for both polarizations exhibit blueshift when increasing the angle of incidence, especially in the case of TE polarization. This phenomenon is attributed to the shift of the photonic stopbands of the dielectric multilayer to larger frequencies when increasing the incident angle.[41] To intuitively present the changing trend, we show the frequencies of the resonant peaks and peak absorption versus incident angle in Fig. 4(c) and Fig. 4(d), respectively. As depicted in Fig. 4(c), the frequencies of the resonant peaks for both TE-polarized and TM-polarized waves remain almost equal with the increase of incident angle from 0° to 30°. Though the differences between the resonant

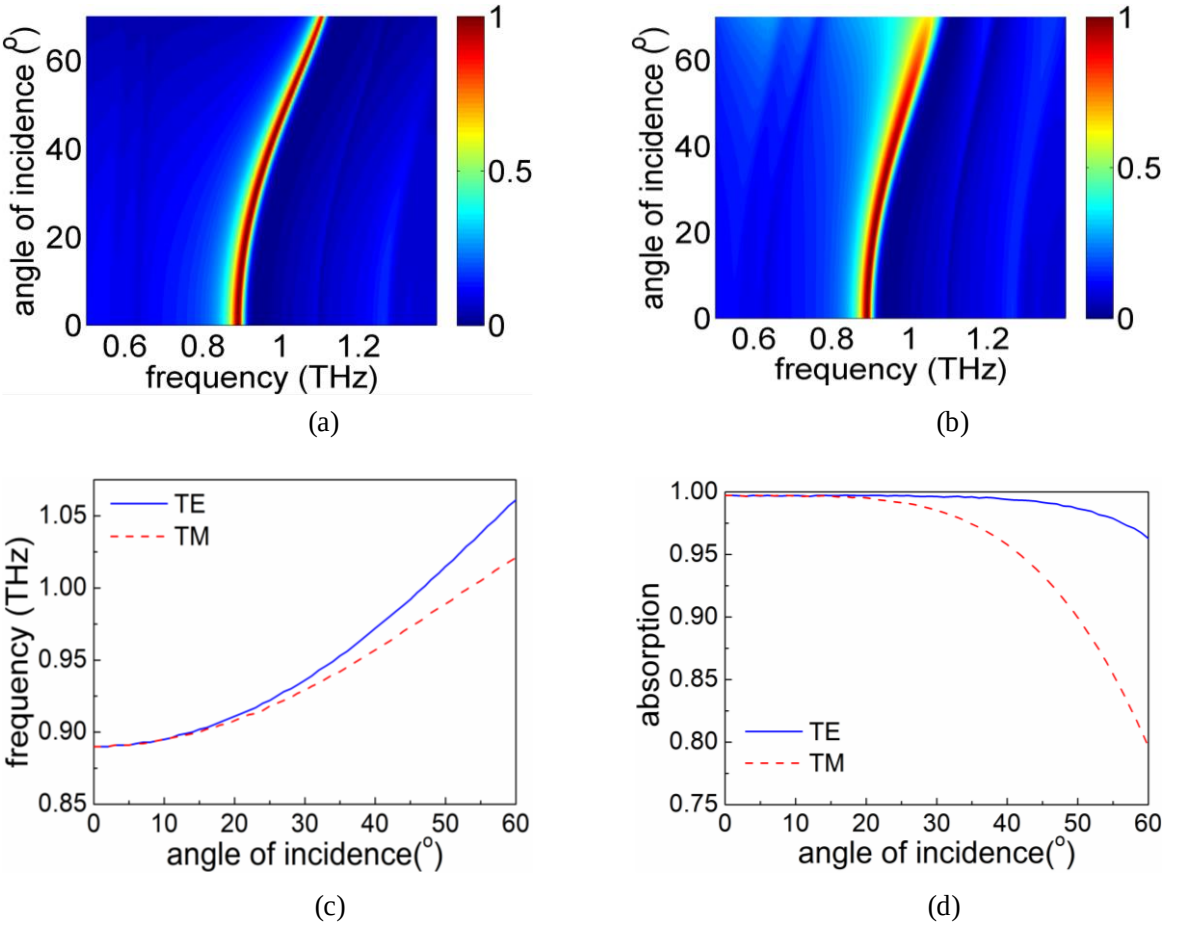

Fig. 4 Light absorption in monolayer graphene versus the change of frequency and incident angle for (a) TE polarization and (b) TM polarization, respectively. (c) Resonant frequency and (d) peak absorption as a function of incident angle for both polarizations, respectively.

the frequency between the two polarizations becomes larger with the incident angle varying from 40° to 70°, their differences are still small enough relative to the resonant frequency. Thus, the proposed absorber can be considered to be insensitive to the polarization state, which is a particular advantage for practical application. The changing trend of the peak absorption versus incident angle is similar to that of the resonant frequency, as shown in Fig. 4(d). Moreover, it is also found that the perfect absorption in monolayer graphene can be maintained in a large incident angle range.

Typically, for the device manufacture, the dimension tolerance of the designed absorber should be taken into account. For this purpose, we show the effects of the structure dimensions on the absorption spectra in Fig. 5. From Fig. 5(a), it is found that increasing h_1 from 100 μm to 110 μm results in redshifts of the absorption peak. However, the profile of the absorption spectra remains unchanged. Figs. 5(b) and 5(c) show that the resonant peaks shift to the smaller frequencies with the increase of h_a or h_b, both of which exhibit a redshift. Moreover, with the same amount of change in h_a and h_b, the

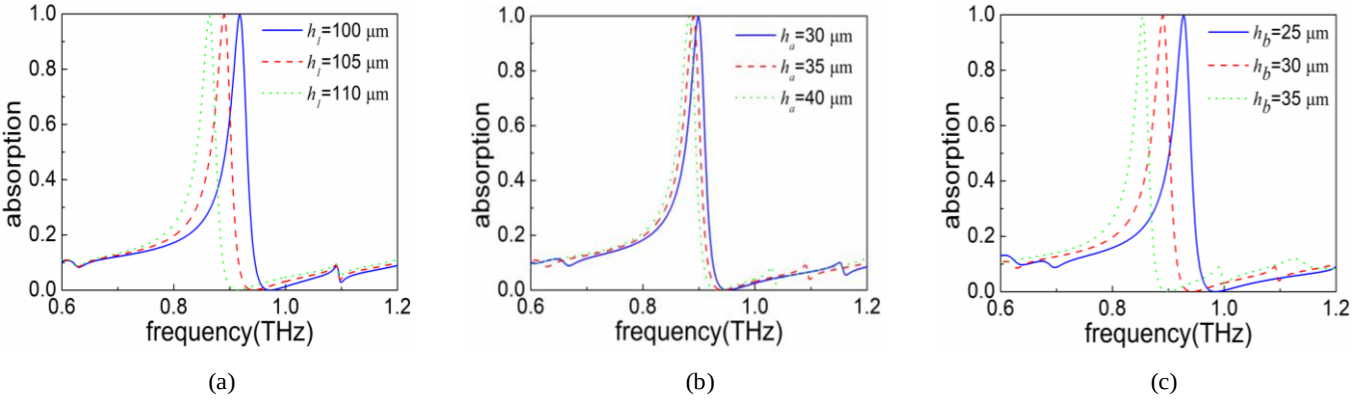

Fig. 5 (a) Absorption in graphene monolayer as a function of (a) h_1, (b) h_a, and (c) h_b.

redshift with the increase of h_b is larger than that of h_a, as the shift of the photonic stopbands with the increase of h_b is larger than that by increasing h_a, which has been explained by a method based on the Fourier Transform of the structure index profile.[42] Clearly, with the change of the geometric parameters, the resonant frequency of the absorption peak can be changed nearly linearly and the absorption performance retains almost unchanged, which can be used to tune the operating frequencies. More importantly, the perfect graphene absorption can be maintained within the relatively large structure dimensions range, benefiting the potential applications of the devices.

Lastly, the dynamically controlling of the perfect absorption through changing the Fermi energy of the graphene is investigated. According to Eq. (1), the conductivity of graphene has a linearly relationship with E_f. Thus, change in E_f will have a direct influence on the absorption spectra. In Fig. 6, we calculate and illustrate the absorption spectra for different E_f. Clearly, increasing the E_f from 0.60 eV to 0.90 eV leads to blue shifts of the absorption peak. More importantly, the absorption property remains almost unchanged. Therefore, the operating frequency can be easily controlled through changing the gate voltage, which is particularly attractive for real application as the absorption properties can be dynamically controlled without re-designing and re-fabricating another new device. For practical application, to change the Fermi energy of the monolayer graphene, two electrodes can be fabricated by thermal deposition, one was on the graphene and the other one was on the dielectric spacer for the gate voltage.

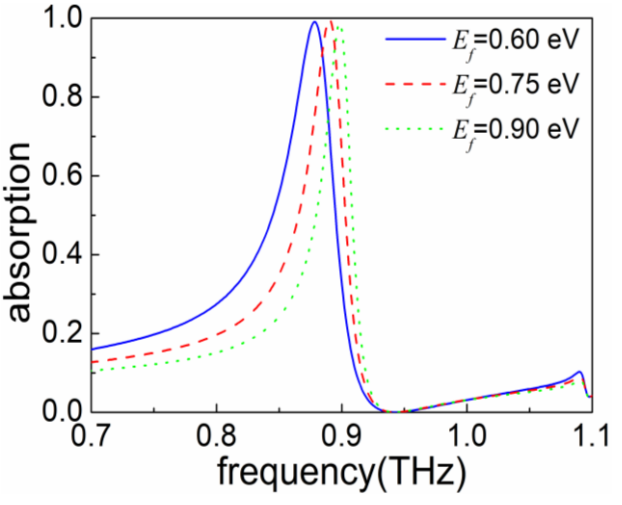

Fig. 6 Absorption spectra versus the change of the Fermi energy of graphene.

4. Conclusions

In conclusion, the perfect absorption effect in monolayer graphene based on graphene-dielectric multilayer structure is investigated. The results show that graphene TPPs with frequency locating at the photonic stopband of the dielectric multilayer can be excited, leading to perfect absorption in monolayer graphene. This phenomenon is intuitively confirmed by the electric field intensity profile along the z-axis, where strongly electric field intensity enhancement is highly confined in the spacer just bellow graphene due to the excitation of the graphene TPPs, which boosts the absorption in graphene. It is also found that the operating frequencies can be flexibly tuned with larger polarization independence by adjusting the angle of incidence. Besides, the absorption properties of the proposed absorber can be maintained with large structure dimension tolerance, which is advantage for practical fabrication. Lastly, it is found that the operating frequency can be flexibly tunable by only a change in the gate-voltage. Our results should have potential applications in the developing of novel tunable devices based on monolayer graphene, including filters, absorber and thermal detectors.

Acknowledgements

The authors acknowledge the support of National Natural Science Foundation of China (61405217), Zhejiang Provincial Natural Science Foundation under Grant No. LY20F050001, Anhui Polytechnic University Research Startup Foundation (Grant No. 2020YQQ042) and the Pre-research project of National Natural Science Foundation of Anhui Polytechnic University (Grant No. Xjky02202003).

Supporting information

Not applicable.

Conflict of interest

There are no conflicts to declare.

References

[1] F. Alves, D. Grbovic, B. Kearney, N. V. Lavrik, G. Karunasiri, *Optics Express*, 2013, **21**, 13256, doi: 10.1364/oe.21.013256.

[2] J. Liu, L. Fan, J. Ku, L. Mao, *Optical and Quantum Electronics*, 2016, **48**, 80, doi: 10.1007/s11082-015-0361-5.

[3] M. Mittendorff, S. Winnerl, J. Kamann, J. Eroms, D. Weiss, H. Schneider, M. Helm, *Applied Physics Letters*, 2013, **103**, 021113, doi: 10.1063/1.4813621.

[4] I. E. Carranza, J. Grant, J. Gough, D. Cumming, *IEEE Journal of Selected Topics In Quantum Electronics*, 2017, 23, 4700508.

[5] S. A. Kuznetsov, A. G. Paulish, A. V. Gelfand, P. A. Lazorskiy, V. N. Fedorinin, *Progress in Electromagnetics Research*, 2012, **122**, 93-103, doi: 10.2528/pier11101401.

[6] K. Iwaszczuk, A. C. Strikwerda, K. Fan, X. Zhang, R. D. Averitt, P. U. Jepsen, *Optics Express*, 2011, **20**, 635, doi: 10.1364/oe.20.000635.

[7] K. Halterman, J. M. Elson, *Optics Express*, 2014, **22**, 7337, doi: 10.1364/oe.22.007337.

[8] R. Kakimi, M. Fujita, M. Nagai, M. Ashida, T. Nagatsuma, *Nature Photonics*, 2014, **8**, 657-663, doi: 10.1038/nphoton.2014.150.

[9] N. I. Landy, S. Sajuyigbe, J. J. Mock, D. R. Smith, W. J. Padilla, *Physical Review Letters*, 2008, **100**, 207402, doi: 10.1103/physrevlett.100.207402.

[10] M. Kenney, J. Grant, Y. D. Shah, I. Escorcia-Carranza, M.

Humphreys, D. R. S. Cumming, *ACS Photonics*, 2017, **4**, 2604-2612, doi: 10.1021/acsphotonics.7b00906.
[11] F. Hu, N. Xu, W. Wang, Y.-E. Wang, W. Zhang, J. Han, W. Zhang, *Journal of Micromechanics and Microengineering*, 2016, **26**, 025006, doi: 10.1088/0960-1317/26/2/025006.
[12] G. Isić, B. Vasić, D. C. Zografopoulos, R. Beccherelli, R. Gajić, *Physical Review Applied*, 2015, **3**, 064007, doi: 10.1103/physrevapplied.3.064007.
[13] L. Ye, Y. Chen, G. Cai, N. Liu, J. Zhu, Z. Song, Q. H. Liu, *Optics Express*, 2017, **25**, 11223, doi: 10.1364/oe.25.011223.
[14] F. Bonaccorso, Z. Sun, T. Hasan, A. C. Ferrari, *Nature Photonics*, 2010, **4**, 611-622, doi: 10.1038/nphoton.2010.186.
[15] A. N. Grigorenko, M. Polini, K. S. Novoselov, *Nature Photonics*, 2012, **6**, 749-758, doi: 10.1038/nphoton.2012.262.
[16] Q. Bao, K. P. Loh, *ACS Nano*, 2012, **6**, 3677-3694, doi: 10.1021/nn300989g.
[17] J. Christensen, A. Manjavacas, S. Thongrattanasiri, F. H. L. Koppens, F. J. García de Abajo, *ACS Nano*, 2012, **6**, 431-440, doi: 10.1021/nn2037626.
[18] F. H. L. Koppens, D. E. Chang, F. J. García de Abajo, *Nano Letters*, 2011, **11**, 3370-3377, doi: 10.1021/nl201771h.
[19] K. F. Mak, M. Y. Sfeir, Y. Wu, C. H. Lui, J. A. Misewich, T. F. Heinz, *Physical Review Letters*, 2008, **101**, 196405, doi: 10.1103/physrevlett.101.196405.
[20] A. Vakil, N. Engheta, *Science*, 2011, **332**, 1291-1294, doi: 10.1126/science.1202691.
[21] S. Thongrattanasiri, F. H. L. Koppens, F. J. García de Abajo, *Physical Review Letters*, 2012, **108**, 047401, doi: 10.1103/physrevlett.108.047401.
[22] R. Alaee, M. Farhat, C. Rockstuhl, F. Lederer, *Optics Express*, 2012, **20**, 28017, doi: 10.1364/oe.20.028017.
[23] F. Xia, T. Mueller, Y.-M. Lin, A. Valdes-Garcia, P. Avouris, *Nature Nanotechnology*, 2009, **4**, 839-843, doi: 10.1038/nnano.2009.292.
[24] J. Liu, P. Li, Y. Chen, X. Song, F. Qi, B. Zheng, J. He, Q. Wen, W. Zhang, *Chinese Optics Letters*, 2016, **14**, 052301, doi: 10.3788/col201614.052301.
[25] B. Sensale-Rodriguez, S. Rafique, R. Yan, M. Zhu, V. Protasenko, D. Jena, L. Liu, H. G. Xing, *Optics Express*, 2013, **21**, 2324, doi: 10.1364/oe.21.002324.
[26] T.-H. Xiao, L. Gan, Z.-Y. Li, *Photonics Research*, 2015, **3**, 300, doi: 10.1364/prj.3.000300.
[27] L. Wu, J. Guo, H. Xu, X. Dai, Y. Xiang, *Photonics Research*, 2016, **4**, 262, doi: 10.1364/prj.4.000262.
[28] Y. Zhang, Y. Feng, B. Zhu, J. Zhao, T. Jiang, *Optics Express*, 2014, **22**, 22743, doi: 10.1364/oe.22.022743.
[29] X. H. Deng, J. T. Liu, J. Yuan, T. B. Wang, N. H. Liu, *Optics Express*, 2014, **22**, 30177, doi: 10.1364/oe.22.030177.
[30] X. He, X. Zhong, F. Lin, W. Shi, *Optical Materials Express*, 2016, **6**, 331, doi: 10.1364/ome.6.000331.
[31] L. Zhu, F. Liu, H. Lin, J. Hu, Z. Yu, X. Wang, S. Fan, *Light: Science & Applications*, 2016, **5**, e16052, doi: 10.1038/lsa.2016.52.
[32] R. M. Gao, Z. C. Xu, C. F. Ding, J. Q. Yao, *Applied Optics*, 2016, **55**, 1929, doi: 10.1364/ao.55.001929.
[33] X. Wang, X. Jiang, Q. You, J. Guo, X. Dai, Y. Xiang, *Photonics Research*, 2017, **5**, 536, doi: 10.1364/prj.5.000536.
[34] V. P. Gusynin, S. G. Sharapov, J. P. Carbotte, *Physical Review Letters*, 2006, **96**, 256802, doi: 10.1103/physrevlett.96.256802.
[35] C. H. Gan, H. S. Chu, E. P. Li, *Physical Review B*, 2012, **85**, 125431, doi: 10.1103/physrevb.85.125431.
[36] M. G. Moharam, E. B. Grann, D. A. Pommet, T. K. Gaylord, *Journal of the Optical Society of America A*, 1995, **12**, 1068–1076, doi: 10.1364/JOSAA.12.001068.
[37] P. Lalanne, G. M. Morris, *Journal of the Optical Society of America A*, 1996, **13**, 779-784, doi: 10.1364/JOSAA.13.000779.
[38] A. V. Kavokin, I. A. Shelykh, G. Malpuech, *Physical Review B*, 2005, **72**, 233102, doi: 10.1103/physrevb.72.233102.
[39] M. Kaliteevski, I. Iorsh, S. Brand, R. A. Abram, J. M. Chamberlain, A. V. Kavokin, I. A. Shelykh, *Physical Review B*, 2007, **76**, 165415, doi: 10.1103/physrevb.76.165415.
[40] S. Brand, M. A. Kaliteevski, R. A. Abram, *Physical Review B*, 2009, **79**, 085416, doi: 10.1103/physrevb.79.085416.
[41] X. Wang, X. Hu, Y. Li, W. Jia, C. Xu, X. Liu, J. Zi, *Applied Physics Letters*, 2002, **80**, 4291-4293, doi: 10.1063/1.1484547.
[42] Y. Gong, X. Liu, L. Wang, H. Lu, G. Wang, *Optics Express*, 2011, **19**, 9759, doi: 10.1364/oe.19.009759.

Author information

Jun Wu *is an associate research fellow of Anhui Polytechnic University, working in nanophotonics, diffractive optics and metasurface. He received Ph.D degree from Shanghai Institute of Optics and Fine Mechanics in 2013. He was once an assistant research fellow from 2013 to 2015 and an associate research fellow from 2015 to 2018, working in Shanghai Institute of Optics and Fine Mechanics. He has published 28 journal and conference papers.*

